Proposed Use of Step Quantum Wells for Terahertz Quantum Cascade Lasers

Will Freeman and Gamani Karunasiri

***Abstract*—Terahertz (THz) quantum cascade lasers (QCLs) have been designed by a number of approaches and variations using square quantum wells. In this paper, a step quantum well structure is analyzed for use in LO-phonon assisted QCLs where the radiative transition and LO-phonon transition are within the same well. The electron-phonon and electron-electron scattering rates are calculated for this step well and a QCL structure for operating in the THz frequencies is proposed.**

***Index Terms*—Step quantum well, terahertz, quantum cascade laser, LO-phonon.**

THE first terahertz QCL by Köhler *et al.*[1] used chirped superlattices. Other designs by Scalari *et al.*[2,3] included a bound to continuum and a bound to continuum with optical-phonon scattering approaches. The first terahertz QCL that used electron-phonon scattering for depopulation similar to that of Faist's *et al.*[4] mid-infrared QCL, was by Williams *et al.*[5]. Variations of the terahertz LO-phonon based designs have essentially been within the same framework. All of these design approaches used square quantum wells, i.e., quantum wells that are symmetric when not under bias.

It is not possible to have an upper radiative terahertz energy spacing and LO-phonon energy spacing within a single square quantum well. A step quantum well, in which two different material compositions are used, breaks this restriction. In a step well, a terahertz and LO-phonon energy spacing can be arranged within a single step quantum well. This approach is illustrated in Figure 1. The well is comprised of $Al_xGa_{1-x}As$ layers with compositions of 0.143/0.035/0/0.143, where the material parameters given Vurgaftman *et al.*[6] have been used. The step well thicknesses in nm are 20.9/13.5, and the radiative energy spacing is E_{21} = 17.9 meV (4.3 THz). The 1 to 0 transition has E_{10} = 36.5 meV which is near the LO-phonon energy. An applied field of 10.1 kV/cm was applied, which is typical for LO-phonon QCLs. This illustrates that it is possible to arrange the upper radiative transition and near resonant phonon transition in the same step well. This approach can be used to engineer radiative frequencies lower and higher than the 4.2 THz value as well.

While intrawell radiative transitions can have large overlap of the electron wavefunctions which yield large oscillator strengths, there can be a trade off between the oscillator strength and upper state lifetime as the parasitic scattering from the upper radiative state to the ground state can be increased. The necessary condition at steady state for a population inversion to exist ($n_2 > n_1$) is $W_{10} > W_{21}$ (in terms of corresponding lifetimes $\tau_{10} < \tau_{21}$). In general, the scattering rates are a combination of all possible scattering mechanisms, i.e., electron-phonon, electron-electron, impurity, and interface roughness scattering. The scattering rates were estimated by taking into account the electron-phonon and electron-electron scattering rates.

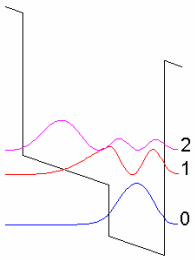

Fig. 1. Conduction band profile of a step quantum well comprised of $Al_xGa_{1-x}As$ layers with compositions of 0.143/0.035/0/0.143 and well thicknesses in nm of 20.9/13.5. The radiative transition is from 2 to 1 and the 1 to 0 transition is near the LO-phonon energy.

The Fröhlich[7] interaction for the electron-phonon scattering was computed using the bulk phonon interaction potential. The mean scattering rate is calculated by averaging over the Fermi-Dirac distribution of carriers in the initial state. The mean electron-phonon scattering rates for the 4.3 THz step quantum well in Figure 1 were calculated for initial state populations from 1×10^9 cm^{-2} to 1×10^{10} cm^{-2} for $T_{lattice}$ = 25 K and $T_{electron}$ = 100 K. All of the scattering rates are essentially constant and independent across the populations computed. The corresponding rate lifetimes computed are τ_{10} = 0.37, τ_{21} = 5.6 psec, and τ_{20} = 1.8 psec. Since τ_{21} = 5.6 psec > τ_{10} = 0.37 psec, this indicates that the electron-phonon rates are favorable for keeping a population inversion.

The electron-electron scattering rates due to antiparallel spin electrons[8-13] were calculated for the same 4.3 THz structure as for the electron-phonon analysis, noting that including parallel spin collisions with the exchange term produces a lower scattering rate. The rates were computed again for initial state populations from 1×10^9 cm^{-2} to 1×10^{10} cm^{-2} using $T_{electron}$ = 100 K. The dominant scattering rate is from the 2010 process. The electron-electron scattering rates are not constant, but rather as expected increases with carrier concentration. The total electron-electron scattering rates are the sum of the various processes taking into account the number of electrons that change energy levels. The total electron-electron scattering rates by themselves are not favorable for a population inversion. However, since they are an order of magnitude less than the electron-phonon scattering

Manuscript received August 29, 2007. This work was supported by NAVAIR's In-House Independent Research (ILIR) Program under the auspices of the Office of Naval Research (ONR). One of us (G.K.) would like to acknowledge the support of AFOSR.

W. Freeman is with the Naval Air Warfare Center, Physics and Computational Sciences Division, China Lake, CA 93555 USA.

G. Karunasiri is with the Department of Physics, Naval Postgraduate School, Monterey, CA 93943 USA.

rates, this indicates this type of structure is capable of keeping a population inversion for these temperatures and range of carrier concentrations.

In order for the step quantum well to be used in a quantum cascade laser, an injector section must be included to feed the next module. Illustrated in Figure 2 (where one module is outlined) is one such proposed structure. The step well has been shaped in an effort to reduce the parasitic scattering from the upper state 4 to the triplet states (2, 1, 0), by shoving the upper state wavefunction as much as possible to the left inside the well. The radiative transition takes place between states 4 and 3, where E_{43} = 17.3 meV (4.2 THz or λ ~ 72 μm). The LO-phonon assisted transition primarily takes place from states 3 to 1 since E_{31} = 37.3 meV which is near $\hbar\omega_{LO}$. Phonon transitions can also take place from states 3 to 0 and states 3 to 2, with the later rate being reduced because the energy separation is less than $\hbar\omega_{LO}$. In this approach, mini-band scattering between the triplet of ground states is to take place, and then injection from state 0 to state 4 of the adjacent module. The step well has been arranged so that state 4 is above the step and the state 3 below it, in an attempt to minimize unwanted injection to state 3 from the previous modules ground state.

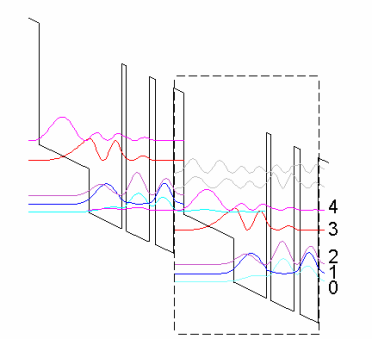

Fig. 2. Conduction band profile of a proposed step well quantum cascade laser found using a self-consistent solution to the Schrödinger and Poisson equations. The step well and resonant tunneling double barriers of one module are outlined. Beginning with the left injector, the $Al_xGa_{1-x}As$ layers compositions are 0.143/0.035/0/0.143/0/0.143/0 and thicknesses in nm are 4.3/20.9/13.5/1.7/9.6/2.5/7.6. The radiative transition is from 4 to 3 and the 3 to 1 transition is near the LO-phonon energy. The applied field is 10.1 kV/cm and the 9.6 nm well is doped 2.9×10^{16} cm^{-3} which corresponds to a sheet density of 2.8×10^{10} cm^{-2}.

The electron-phonon scattering from 3 to (2, 1, 0) gives a lifetime of ~ 0.4 psec. The radiative transition is also an intrawell transition, and the overlap of the wavefunctions is reasonably good which gives an oscillator strength of about 1.52. This oscillator strength is somewhat higher than the ~ 1 oscillator strength of most of the other LO-phonon designs[5] and more close to that of the bound continuum designs[2,3]. The parasitic scattering rate is also higher at ~ 1.4 psec. The 2D population inversion can be estimated using

$$gain = \frac{2e^2\hbar^2\Delta n_{3D}}{m^2\,\varepsilon\, n_{index}\, c\,\omega\, FWHM}\left|\langle f|\frac{d}{dx}|i\rangle\right|^2 \qquad (1)$$

where Δn_{3D} is the 3D population inversion and n_{index} is the index of refraction. Assuming a total loss of ~ 41 cm^{-1} (which is reasonable for the surface plasmon waveguides) and assuming a *FWHM* ~ 4 meV, the estimated 2D population at threshold approximating the lower state as empty is 2.7×10^{9} cm^{-2}. This is within the carrier densities used in our analysis. The actual carrier concentration may be higher since the lower state will not be completely empty. The total upper radiative state 4 lifetime is estimated to be about 0.56 psec. The parasitic scattering rate from state 4 to (2, 1, 0) and the tunneling rate to the continuum, were used in this calculation. This implies that tunneling rather than the relatively fast parasitic scattering rate of 1.4 psec from state 4 to (2, 1, 0) is what dominates the total upper state lifetime. Similar tunneling rates from the upper state were found from previously reported QCL structures[5]. The current density is estimated from $\Delta n_{2D} \sim (J/e)\ \tau_4\ (1 - \tau_3/\ \tau_{4,3})$ to be $J \sim 810$ A/cm^{-2}.

In summary, our analysis indicates that step quantum wells may be capable of maintaining a population inversion for low carrier concentrations expected in QCLs. A full structure that uses a step well and a double barrier section for injection to the next module has been proposed. The vertical nature of the radiative transition yields a relatively high oscillator strength, and also an increased parasitic scattering rate from the upper state to the ground states. Further analysis is needed to see if such structures are practical for QCL devices and to accurately determine the electron temperatures and subband populations of the full structure.

REFERENCES

[1] R. Köhler, A. Tredicucci, F. Beltram, H. E. Beere, E. H. Linfield, A. G. Davies, D. A. Ritchie, R. C. Iotti, and F. Rossi. Terahertz semiconductor-heterostructure laser. *Nature*, 417:156, 2002.

[2] G. Scalari, L. Ajili, J. Faist, H. Beere, E. Linfield, D. Ritchie, and G. Davies. Far-infrared (λ ≈ 87μm) bound-to-continuum quantum- cascade lasers operating up to 90 K. *Appl. Phys. Lett.*, 82:3165, 2003.

[3] G. Scalari, N. Hoyler, M. Giovannini, and J. Faist. Terahertz bound-to-continuum quantum-cascade lasers based on optical-phonon scattering extraction. *Appl. Phys. Lett.* 86:181101, 2005.

[4] J. Faist, F. Capasso, D. L. Sivco, C. Sirtori, A. L. Hutchinson, and A. Y. Cho. Quantum cascade laser. *Science*, 264:553, 1994.

[5] B. S. Williams, H. Callebaut, S. Kumar, Q. Hu, and J. L. Reno. 3.4-THz quantum cascade laser based on longitudinal-optical-phonon scattering for de-population. *Appl. Phys. Lett.*, 82:1015, 2003.

[6] I. Vurgaftman, J. R. Meyer, and L. R. Ram-Mohan. Band parameters for III-V compound semiconductors and their alloys. *J. Appl. Phys.*89:5815, 2001.

[7] H. Fröhlich, Theory of Electrical Breakdown in Ionic Crystals. *Proc. Roy. Soc.* A 160, 230, 1937.

[8] S. M. Goodnick and P. Lugli, Effect of electron-electron scattering on nonequilibrium transport in quantum-well systems. *Phys. Rev. B,* 37: 2578, 1988.

[9] M. Mosko, A. Moskova, and V. Cambel, Carrier-carrier scattering in photoexcited intrinsic GaAs quantum wells and its effect on femtosecond plasma thermalization. *Phys. Rev. B,* 51: 16860, 1995.

[10] A. Tomita, J. Shah, J. E. Cunningham, S. M. Goodnick, P. Lugli, and S. L. Chuang, Erratum: Femtosecond hole relaxation in *n*-type modulation-doped quantum wells [Phys. Rev. B 48, 5708 (1993)]. *Phys. Rev. B,* 52: 5445, 1995.

[11] T. Ando, A. B. Fowler, and F. Stern, Electronic properties of two-dimensional systems. *Rev. Mod. Phys.*, 54:437, 1982.

[12] J. H. Smet, C. G. Fonstad, and Q. Hu. Intrawell and interwell intersubband transitions in multiple quantum wells for far-infrared sources. *J. Appl. Phys.*, 79:9305, 1996.

[13] *Quantum Wells Wires, and Dots*, 2nd editon, P. Harrison, Wiley, 2006.